

Original Research Article

Open Access

Land Use/Land Cover Mapping Using Multi-temporal Sentinel-2 Imagery—A Case Study from Ramganga River Sub-basin



Hari Krishna B¹, Susama Sudhishri^{2*}, Debasish Roy³, Man Singh², Manoj Khanna², P. S. Bramhanand², D. K. Singh², R. N. Sahoo⁴, Dinesh Kumar⁵, V. K. Sharma⁶, Ravi teja Machanuru⁷, A. Sairam², and Sidhartha Gaddam²

¹Department of Agronomy, Professor Jayashankar Telangana Agricultural University, Agricultural College- Warangal, Telangana-506007, India

²Water Technology Centre, ICAR- Indian Agricultural Research Institute, New Delhi- 110012, India

³India Meteorological Department, New Delhi- 110003, India

⁴Division of Agricultural Physics, ICAR- Indian Agricultural Research Institute, New Delhi- 110012, India

⁵Division of Agronomy, ICAR- Indian Agricultural Research Institute, New Delhi- 110012, India

⁶Division of Soil Science and Agricultural Chemistry, ICAR- Indian Agricultural Research Institute, New Delhi- 110012, India

⁷School of Natural Resource Management, ICAR- Indian Agricultural Research Institute, Assam- 787035, India

ABSTRACT

Evaluation of river basins requires land-use and land-cover (LULC) change detection to determine hydrological and ecological conditions for sustainable use of their resources. This study investigates the changes in cropping patterns, classification accuracy, and land use patterns during the kharif and rabi seasons of 2018-19. The supervised classification, employing the maximum likelihood classifier method, was used to generate the classified LULC maps in the ERDAS Imagine. The classified images produced by this technique were evaluated for accuracy through matrix union using the statistical kappa coefficient and overall accuracy measures. Change detection for the periods 2018-19 was conducted using matrix union (intersection) to identify apparent changes in various LULC classes. The analysis shows a significant shift in cropping practices, particularly a notable transition from rice to wheat during the rabi season, with wheat cultivation increasing by 75.53%. Other crops such as mustard, vegetable pea, and sugarcane also saw significant changes in acreage, reflecting farmers' responses to market and climatic conditions. Soybean, traditionally grown during the kharif season, shifted to wheat in the rabi season. The classification accuracy for both kharif and rabi crops was high, with overall accuracies of 92.95% and 94.02%, respectively, and Kappa coefficients of 89.98% and 92.81%, indicating reliable classification results. Key challenges included resolving spectral confusion between crops (e.g., wheat vs. mustard) and addressing cloud cover limitations in kharif-season imagery. The study's contributions include: (1) a robust framework for high-resolution crop monitoring in heterogeneous landscapes, (2) quantification of rapid cropping system transitions, and (3) demonstration of Sentinel-2's operational utility for precision agriculture. Results support evidence-based policymaking for sustainable water and land use in monsoon-dependent systems.

Keywords: Land use land cover; River subbasin; Sentinel-2, Maximum likelihood classification

Introduction

Land cover refers to the physical state of the Earth's surface and its biological elements, while land use describes how this land cover is altered by human activities to meet specific needs and purposes [1]. In remote sensing, change detection is one of the major applications of remotely sensed data obtained from earth-orbiting satellites. Several studies have been conducted on the surface of earth to assess, monitor, and evaluate LULC change information coupled with the historical remotely sensed data because of repetitive coverage at short intervals [2],[3],[4]. In recent years, the growth of human activities could greatly contribute to understanding the dynamics and patterns of land use and land cover changes [5],[6],[7].

In addition, LULC investigation has the potential to greatly impact natural resource management[8]. The accurate and sufficient information regarding LULC has become vital for determining the social, economic, and environmental repercussions of such changes and for understanding those repercussions [9]. The rapid urban population growth strains urban infrastructure, resulting in a low people-to-land ratio and, as a result, land degradation. Recently, it has become necessary to evaluate changes in LULC to carry out appropriate planning and ensure natural resources are protected in various ways by utilizing geospatial technology [10].

In the domains of hydrometeorology, climate change, and environmental studies, remote sensing (RS) and geographic information systems (GIS) have been employed for a wide range of applications. While RS provides high-resolution spatial data, GIS offers specialized tools for more efficient environmental and ecosystem management [11]. One common technique for quantifying land use and land cover (LULC) is change detection analysis, which often utilizes multi-spectral RS data. Multi-spectral and multi-temporal RS satellite data have opened up

*Corresponding Author: **Susama Sudhishri**

DOI: <https://doi.org/10.21276/AATCCReview.2025.13.02.165>

© 2025 by the authors. The license of AATCC Review. This article is an open access article distributed under the terms and conditions of the Creative Commons Attribution (CC BY) license (<http://creativecommons.org/licenses/by/4.0/>).

numerous research possibilities, including the exploration of LULC patterns. A variety of Landsat imagery, such as data from the Landsat Operational Land Imager (OLI), Thermal Infrared Sensor (TIRS), Enhanced Thematic Mapper Plus (ETM+), Thematic Mapper (TM), and Multi-Spectral Scanner (MSS), have been instrumental in examining LULC changes[12]. These images also provide valuable insights into regular crop monitoring and various agricultural or environmental indices. Moreover, RS data has facilitated local environmental studies and supported LULC change management and conservation efforts at global, regional, and local levels. Various methods used to detect LULC changes include the use of remote sensing (RS) data, cross-correlation analysis, image differencing, post-classification comparison (PCC), object- and pixel-based classification techniques for mapping LULC changes, and image fusion approaches for detecting these changes[13],[14].

Most methods for spectral classification of remotely sensed images are based on per-pixel approaches, which have been applied with varying levels of success, largely depending on the spatial uniformity of the land cover being mapped. For change detection, algorithms typically use a post-classification comparison (PCC) or, less frequently, an image-to-image comparison that assesses spectral changes between different dates[15], [16]. However, one significant drawback of these methods, which is compounded by the limitations of per-pixel classifiers, is the potential for recording false changes due to inaccuracies in land-use maps for individual years[17],[18]. To effectively monitor these changes, it is essential to produce reliable and accurate LULC maps. The information derived from these maps is vital for various areas such as policy development, conservation planning, urban development, deforestation management, and agricultural monitoring. Thanks to advanced remote sensing technologies, these changes can now be tracked at multiple scales[19]. The objective of this study is 1) to analyze land-use and land-cover (LULC) changes within a river basin necessary for the sustainable management of its resources. 2) to investigate changes in cropping patterns, evaluate the accuracy of classification methods, and track land use during the kharif and rabi seasons of 2018-19.

Materials and Methods

Site Descriptions

The study area, Ramganga River sub-basin extended an area 2584 across the Nainital and Udham Singh Nagar districts of Uttarakhand and the Rampur and Bareilly districts of Uttar Pradesh (Fig.1). It is located in between the longitudes 79°1'19.254" E to 79°31'32.97" E, latitudes 28°30'51.9156" N to 29°26'28.0176" N and altitude ranges from 172 m to 2631 m above mean sea level (MSL).

Satellite data

Data collection

Sentinel-2 Level-2 products which provide bottom-of-atmosphere (BOA) reflectance images at 10 m, 20 m and ~10 days temporal resolution was acquired from the ESA platform (<https://scihub.copernicus.eu/dhus/#/home>). For the study, we used blue, green, red and NIR (B2, B3, B4, and B8) at 10 m; Vegetation red edge (B5, B6, B7, B8A) and SWIR (B11 and B12) at 20 m resolution. The satellite data were acquired in 19th, 29th September, and 4th October, 2018 during kharif; 28th December, 2018, 10th January, 2019 and 23rd January, 2019 spanning for rabi seasons. A set of total 6 level-2 S2 cloud-free images were selected for this study.

The detail on satellite sensors, data products, and dates of acquisition is listed in Table 1.

Data pre-processing and classification

To achieve accurate surface information from satellite data, it is essential to apply radiometric and atmospheric corrections. Radiometric and atmospheric corrections were performed using the ArcGIS 10.6 platform prior to the classification. The imagery scenes were then mosaicked, and the study area was extracted. Our study combined various bands such as RGB B4, B3, B2, NIR B8, vegetation red edge (B5, B6, B7, and B8A), SWIR (B11 and B12) to facilitate the gathering of training data required for the classification of the images. The use of supervised classification required the collection of training data for LULC classes. This is the most important and difficult stage of the supervised categorization process. Using visual interpretation, training areas for each class were drawn with polygons, and the Maximum likelihood classifier was used for classification (Fig. 2). It assumes that radiometric values within each class follow a normal distribution, allowing each class to be characterized using a probability function given by its mean vector and variance-covariance matrix.

Accuracy Evaluation

It is important to perform an accuracy assessment between reference data and classified data. The accuracy of 2018 and 2019 LULC maps was assessed by independent datasets. The kappa coefficient, overall accuracy, and producer's and user's accuracy were calculated from the error matrix. The error matrix is the most widely used and recognized tool for presenting accurate results [20],[21]. Commission error (also referred to as user's accuracy) and omission error (or producer's accuracy) assess the likelihood that a given cell value matches the actual ground truth data and the generated classification, respectively. The overall classification accuracy provides a summary of the degree of agreement or disagreement between the classified data and the reference ground information about land use[22].

This paper assessed quantitative accuracy using sampling procedures. First, we generated a shapefile test data with 1443 points. A confusion matrix is used for assessing accuracy. The calculation involves selecting a sample from a specific class in a categorized map and validating it against the field. The field data is used for the accuracy assessment for the years 2018 and 2019, the classification results of the Sentinel-2A satellite images. The classification accuracy of each method was evaluated based on overall accuracy and the kappa coefficient (derived from the confusion matrix).

$$\text{User's accuracy} = \frac{\text{Number of Correctly Classified Pixels in each Category}}{\text{Total Number of Reference Pixels in that Category (The Row Total)}} \times 100 \tag{1}$$

$$\text{Producer accuracy} = \frac{\text{Number of Correctly Classified Pixels in each Category}}{\text{Total Number of Reference Pixels in that Category (The Column Total)}} \times 100 \tag{2}$$

$$\text{Overall accuracy} = \frac{\text{Total Number of Correctly Classified Pixel (Diagonal)(TCS)}}{\text{Total Number of Reference Pixels (TS)}} \times 100 \tag{3}$$

$$\text{Kappa Coefficient (T)} = \frac{(TS \times TCS) - \sum(\text{Column Total} \times \text{Row Total})}{TS^2 - \sum(\text{Column Total} \times \text{Row Total})} \times 100 \tag{4}$$

Results and Discussions

Classification of major LULC

About 8 and 11 classes were classified during *kharif* and *rabi* crop season (Fig.3). For kharif, rice is the dominant crop cultivated on a Ramganga river subbasin followed by sugarcane along with sparsely cultivated soybean and vegetables like, tomato.

Similarly, during rabi season the wheat as cultivated as major crop over the river basin followed by sugarcane crop. Moreover, mustard, vegetable pea, potato and tomato were grown sparsely along with wheat crop, respectively.

Accuracy assessment

Accuracy assessment is a critical aspect of Land Use/Land Cover (LULC) classification studies [23]. The reliability of classification results is only ensured after performing thorough accuracy checks, as LULC maps derived from satellite imagery can contain errors due to factors like classification techniques and satellite data retrieval methods [24]. In this study, we employed the maximum likelihood classification supervised learning method to perform classification land cover over both kharif and rabi season. The accuracy of the Land Use/Land Cover (LULC) classification was assessed using an error matrix, which compares the classified data with reference ground truth data. The combination of texture and coherence features alone can yield satisfactory classification results, achieving an overall accuracy of 91.55% a kappa coefficient of 89.35% [25]. In this study results show an overall classification accuracy of 92.95%, indicating a high level of agreement between the classified map and the actual ground data. Kappa coefficient of 89.98% further confirms excellent classification quality, suggesting minimal chance agreement (Table. 2). Commission errors (CE) and omission errors (OE) were evaluated for each class. Rice and sugarcane exhibited relatively low commission errors (5.78% and 7.14%, respectively) and high user accuracy (94.22% and 92.86%), indicating strong classification performance. Classes such as tomato and soybean showed higher commission errors (12.77% and 12.10%), indicating more frequent misclassification, but their user accuracies remained acceptable at 87.23% and 87.90%, respectively. For Built-up and Forest areas, commission errors were low, and both classes showed high producer and user accuracies, demonstrating reliable classification. The Water class had a perfect user accuracy of 100%, with no commission errors, highlighting flawless classification for this class. The Producer's Accuracy (PA) ranged from 78.10% (tomato) to 97.96% (rice), indicating that most land cover types were correctly identified by the classification method, though some classes like tomato and scrub showed relatively lower accuracy. Overall, the classification achieved a high level of reliability, with the main sources of error being misclassifications in tomato and soybean. However, the accuracy levels for all classes are deemed sufficient for practical land-use mapping applications.

Likely, during rabi season crop classification using remote sensing data achieved an overall accuracy of 94.02% and a Kappa coefficient of 92.81%, indicating strong agreement with ground truth data (Table. 3). Crops like, wheat and scrub had the highest user accuracies (96.19% and 97.83%, respectively) and low commission errors, reflecting excellent classification performance. While most crops showed strong results, with user accuracies ranging from 91.09% to 94.19%, chilli and tomato exhibited slightly higher commission errors (10% and 8.53%), though their accuracies remained acceptable. Overall, the classification model performed well, accurately distinguishing most rabi crops, with minor room for improvement in some classes.

Change detection of LULC

The cropping pattern shift from kharif to rabi season in 2018-19 highlights significant changes in agricultural land use, driven by seasonal and environmental factors (Fig 4 & Table 4).

Rice, the dominant kharif crop, exhibited considerable transitions to various rabi crops, reflecting a change in farming priorities and agricultural strategies. The most notable shift was from rice to wheat, which saw a substantial increase of 75.53% in area, totaling 82,001.76 ha. The land use/land cover analysis revealed that supervised classification using the maximum likelihood method is more accurate [26]. In this study, the maximum likelihood classifier outperformed the classifying rice, sugarcane, built-up land, and forest areas. This dramatic shift indicates a stronger emphasis on wheat cultivation during the rabi season, possibly due to its higher market demand or favorable climatic conditions. The conversion of rice fields to wheat was a major factor influencing overall cropping patterns, as wheat is a staple rabi crop that thrives under cooler temperatures. This large-scale transition underscores wheat's economic importance in the region and its adaptability to the changing weather patterns during the rabi season.

Other significant transitions from rice to mustard (8.63%, 9,369.53 ha) and rice to vegetable pea (14.14%, 15,346.12 ha) also played an important role in restructuring the cropping landscape. Mustard, an oilseed crop, saw a noticeable increase, highlighting the rising demand for edible oils in the region, as well as the suitability of mustard for cooler rabi conditions. The conversion to vegetable peas suggests a growing trend toward pulse cultivation, which can enrich soil quality by fixing nitrogen, a critical practice in sustainable farming. Additionally, shifts from rice to potato (1.08%, 1,176.24 ha) and rice to sugarcane (0.08%, 84.89 ha) show the diversification of cropping systems. While the area under potato remained relatively small, it points to the adaptability of potato farming in areas with favorable irrigation and soil conditions. The conversion to sugarcane, though minimal, reflects its economic potential in certain regions, where its processing offers a steady income through sugar production.

In contrast, soybean also experienced a significant shift, with the area under this crop transitioning predominantly to wheat (88.25%, 2,025.05 ha) during the rabi season [27]. This suggests that farmers may have been influenced by the profitability and demand for wheat, leading to a large-scale replacement of soybean fields. Sugarcane showed a notable internal shift within the same crop category, with sugarcane to sugarcane (93.30%, 29,707.46 ha), highlighting a consolidation of sugarcane farming during the rabi season, likely driven by favorable irrigation and market factors (Table.4). Additionally, sugarcane to scrub (6.70%, 2,134.64 ha) indicates some land being left uncultivated or shifting towards less intensive farming practices. Overall, the changes in cropping patterns between kharif and rabi seasons in 2018-19 reflect evolving agricultural practices, influenced by factors such as market demand, climate conditions, and crop profitability. These shifts are critical in understanding the region agricultural economy and the challenges faced by farmers in adapting to changing conditions.

Conclusions

In conclusion, the cropping pattern analysis for the kharif and rabi seasons of 2018-19 reveals key shifts in agricultural practices. There was a significant transition from rice to wheat, with wheat acreage increasing by 75.53% during the rabi season. Other shifts included the expansion of mustard, vegetable pea, and sugarcane, demonstrating farmers' responsiveness to market and climatic factors. Soybean also moved towards wheat cultivation, highlighting a trend towards more profitable crops. The classification accuracy was high, with overall accuracies of 92.95% for kharif and 94.02% for rabi,

accompanied by strong Kappa coefficients, indicating minimal misclassification. Despite some errors in specific classes like scrub and tomato, the overall maximum likelihood classification of the model proved reliable. These findings underscore the role of remote sensing in monitoring cropping patterns, offering valuable insights for agricultural management, sustainability, and future crop planning.

Future Scope

Further research could extend this work through long-term multi-decadal LULC trend analysis, integration of machine learning (e.g., Random Forest, CNN) for improved crop classification, and drone-based validation to enhance accuracy in cloud-prone areas. Additionally, investigating socioeconomic drivers (e.g., market prices, policies) behind cropping shifts, coupling LULC data with hydrological models (e.g., SWAT) to assess basin-scale impacts, and developing real-time Sentinel-2 monitoring systems would significantly advance precision agriculture and sustainable land-use planning.

Acknowledgments

The authors are grateful to the Director and Dean of ICAR-IARI, New Delhi for granting a fellowship to H.K.B and the Project Director and Professor of Water Technology Centre, ICAR-IARI, New Delhi for providing the necessary facilities and project staff during the research program.

Author contributions

All the authors contributed intellectual input and research assistance to this study and manuscript preparation. ; H. K. B., S. S., M.S. and M. K. Conceptualization; H. K. B., S. S., D.R., M.S., M. K. and P. S. B. investigation; H. K. B., S. S., D.R., M.S., M. K., P. S. B., D.K. S., R.N. S., D. K., V. K. S., R. M., A. S. and S. G. Methodology, validation, formal analysis and data curation; H. K. B., S. S., D.R., M.S., M. K. and P. S. B., writing; H. K. B., S. S., D.R., M.S., M. K., P. S. B. and R. M. review and editing; S.S. M.S. and M. K. supervision.

Conflict of Interests

The authors declare that the research was conducted in the absence of any commercial or financial relationships that could be construed as a potential conflict of interest.

Data Availability Statement

The original contributions presented in the study are included in the article material, further inquiries are can be directed to the corresponding author.

Figure 1. Study area of Ramganga river subbasin

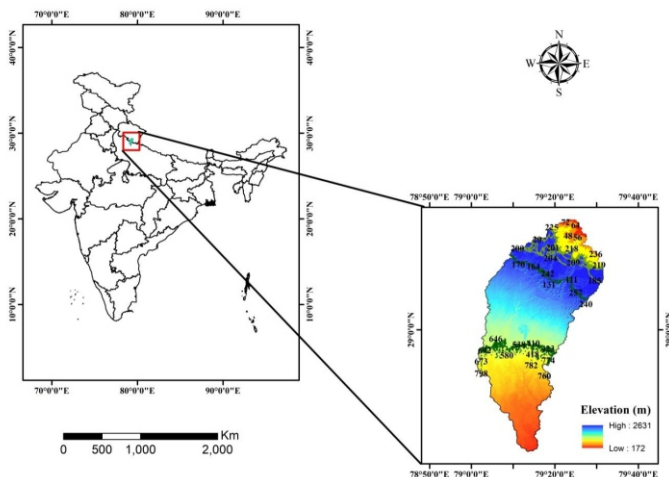


Figure 2. Methodology for develop LULC map using supervised classification

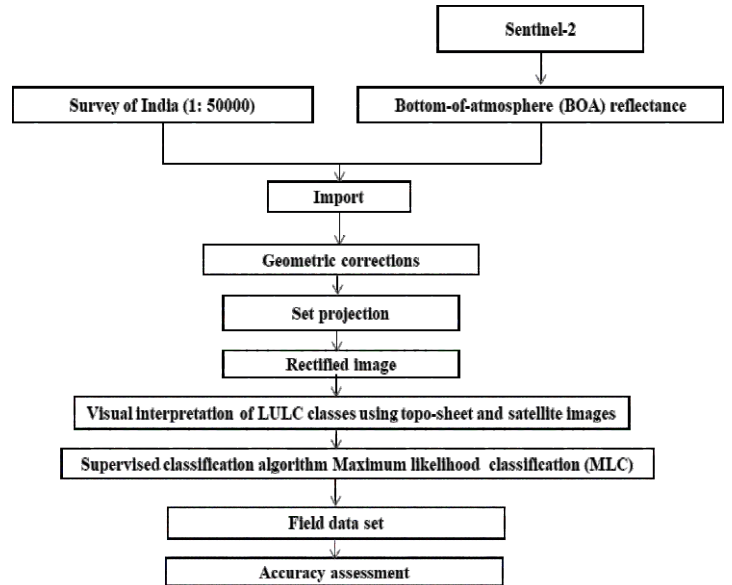


Figure 3. Classified map of Land use land cover (LULC) during Kharif and Rabi season 2018-19

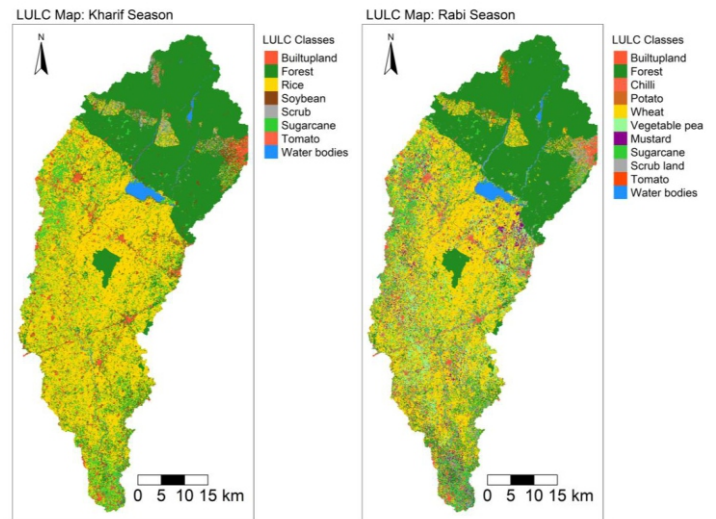


Figure 4. Change detection of LULC from kharif to rabi season

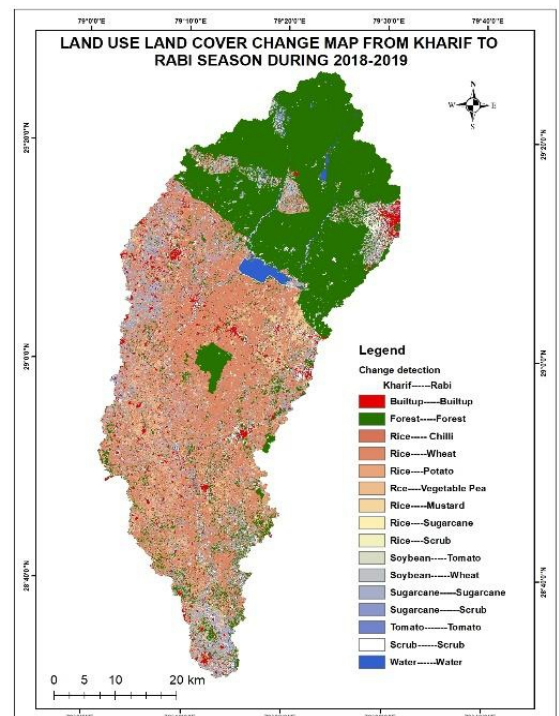


Table 1. Details of satellite data used in this study

Satellite data	Seasons	Date of satellite pass	Resolution (m)	Bands
Sentinel-2	Khari f	19th, 29th September; 4th October, 2018	10 and 20	Blue, Green, Red and NIR (B2, B3, B4, B8) Vegetation Red Edge (B5, B6, B7 and B8A), SWIR (B11 and B12)
	Rabi	28th December, 2018; 10th Jan and 23rd March, 2019		

Table 2. Error matrix for kharif season

Class	Rice	Sugarcane	Tomato	Soybean	Built-up	Forest	Scrub	Water	Total	CE (%)	CE (%)
Rice	815	16	11	8	0	12	2	1	865	5.78	6.78
Sugarcane	8	312	3	5	0	5	2	1	336	7.14	8.14
Tomato	3	2	82	2	1	4	0	0	94	12.77	13.77
Soybean	2	3	6	109	0	2	2	0	124	12.1	13.1
Built-up	0	0	0	0	31	3	0	0	34	8.82	9.82
Forest	4	2	3	1	0	165	3	1	179	7.82	8.82
Scrub	0	0	0	0	3	2	34	0	39	12.82	13.82
Water	0	0	0	0	0	0	0	73	73	0	1
Total	832	335	105	125	35	193	43	76	1744		
OE (%)	2.04	6.87	21.9	12.8	11.43	14.51	20.93	3.95			
PA (%)	97.96	93.13	78.1	87.2	88.57	85.49	79.07	96.05			
Overall Accuracy=92.95%, Kappa Co-efficient=89.98%											

Table 3. Error matrix of rabi crop

Class	Chilli	Potato	Wheat	Vegetable Pea	Mustard	Sugarcane	Scrub	Tomato	Total	CE (%)	UA (%)
Chilli	36	1	1	1	1	0	0	0	40	10	90
Potato	0	92	2	3	3	1	0	0	101	8.91	91.09
Wheat	1	2	379	2	3	5	0	2	394	3.81	96.19
Vegetable Pea	1	2	2	227	3	5	0	1	241	5.81	94.19
Mustard	0	2	3	5	181	4	1	0	196	7.65	92.35
Sugarcane	1	1	7	3	2	290	0	4	308	5.84	94.16
Scrub	0	0	0	0	0	1	45	0	46	2.17	97.83
Tomato	0	1	3	0	1	3	1	118	129	8.53	91.47
Total	39	101	397	241	194	309	47	125	1455		
OE (%)	7.69	8.91	4.53	5.81	6.7	6.15	4.26	5.6			
PA (%)	92.31	91.09	95.47	94.19	93.3	93.85	95.74	94.4			
Overall Accuracy =94.02%, Kappa Co-efficient = 92.81 %											

Table 4. Cropping pattern change under kharif and rabi seasons of 2018-19

Kharif Crops	Rabi Crops	Area (ha)	Change (%)
Rice	Chilli	569.35	0.524449
Rice	Wheat	82001.76	75.53475
Rice	Potato	1176.24	1.083477
Rice	Vegetable pea	15346.12	14.13586
Rice	Mustard	9369.53	8.630608
Rice	Sugarcane	84.89	0.078195
Rice	Scrub	13.75	0.012666
Soybean	tomato	269.52	11.74599
Soybean	wheat	2025.05	88.25401
Sugarcane	Sugarcane	29707.46	93.29617
Sugarcane	scrub	2134.64	6.703829

References

- Prakasam, C (2010) Land use and land cover change detection through remote sensing approach: A case study of Kodaikanal taluk, Tamil nadu. *International Journal of Geomatics and Geosciences*, 1(2): 150.
- Ingram K, E Knapp, and J W Robinson, (1981) Change detection technique development for improved urbanized area delineation. NASA, Comput. Sci. Corp., Springfield, MD, CSC/TM-81/6087.
- Nelson, R.F (1983) Detecting forest canopy change due to insect activity using Landsat MSS. *Photogrammetric Engineering & Remote Sensing*, 49(9): 1303–1314.
- Singh, A (1984) Tropical forest monitoring using digital Landsat data in Northeastern India.
- Halimi, M, Z Sedighifar, and C Mohammadi (2018) Analyzing spatiotemporal land use/cover dynamic using remote sensing imagery and GIS techniques case: Kan basin of Iran. *GeoJournal*, 83: 1067–1077.
- Pasha, SV, C S Reddy, C S Jha, P V V P Rao, and V K Dadhwal (2016) Assessment of land cover change hotspots in Gulf of Kachchh, India using multi-temporal remote sensing data and GIS. *Journal of Indian Society of Remote Sensing*, 44: 905–913.

7. Thakur P K, S S Samant, R K Verma, A Saini, and M Chauhan (2024) Monitoring forest cover changes and its impact on land surface temperature using geospatial technique in Talra Wildlife Sanctuary, Shimla, India. *Environment, Development and Sustainability*: 1–30.
8. Kantakumar, L N, and P Neelamsetti (2015) Multi-temporal land use classification using hybrid approach. *Egyptian Journal of Remote Sensing and Space Sciences*, 18(2): 289–295.
9. Athick, A S M A, K Shankar, and H R Naqvi (2019) Data on time series analysis of land surface temperature variation in response to vegetation indices in twelve Wereda of Ethiopia using mono window, split window algorithm and spectral radiance model. *Data Brief*, 27: 104773.
10. Kumar P, A Husain, R B Singh, and M Kumar (2018) Impact of land cover change on land surface temperature: A case study of Spiti Valley. *Journal of Mountain Science*, 15(8): 1658–1670.
11. Mukherjee S, S S Rizvi, G Biswas, A K Paswan, S P Vaiphei, et al (2023) Aquatic Eco-systems Under Influence of Climate Change and Anthropogenic Activities: Potential Threats and Its Mitigation Strategies. *Hydrogeochemistry of Aquatic Ecosystems*: 307–331.
12. Sajid M, M Mohsin, M Mobeen, A Rehman, A Rafique, et al (2023) Spatio-temporal analysis of land use change and its driving factors in Layyah, Punjab, Pakistan. *The Nucleus*, 60(1): 15–23.
13. Birhanu, A, I Masih, P Van Der Zaag, J Nyssen and X Cai (2019) Impacts of land use and land cover changes on hydrology of the Gumara catchment, Ethiopia. *Physics and Chemistry of the Earth, Parts A/B/C* 112: 165–174.
14. Yang J, J Sun, Q Ge and X Li (2017). Assessing the impacts of urbanization-associated green space on urban land surface temperature: A case study of Dalian, China. *Urban Forestry and Urban Greening*, 22: 1–10.
15. Thein A M and A N Htwe (2023) Based on Principal Component Analysis of Land Use Land Cover Change Detection Using Landsat Satellite Images (Case study Mandalay City). 2023 IEEE Conference on Computer Applications (ICCA). *IEEE*. p. 147–152.
16. Karandikar A and A Agrawal (2023) Performance analysis of change detection techniques for land use land cover. *International Journal of Electrical and Computer Engineering*. 13(4): 4339–4346.
17. Bill Donatien L M, B B Clobite and M L Meris Midel (2024). Land use land cover change detection using multi-temporal Landsat imagery in the North of Congo Republic: a case study in Sangha region. *Geocarto International*, 39(1): 2425184.
18. Lasko Kand F D O'Neill (2023) Automated method for artificial impervious surface area mapping in temperate, tropical, and arid environments using hyperlocal training data with Sentinel-2 imagery. *IEEE Journal of Selected Topics in Applied Earth Observations and Remote Sensing*.
19. Toth C and G Józskó (2016) Remote sensing platforms and sensors: A survey. *International Society for Photogrammetry and Remote Sensing Journal of Photogrammetry and Remote Sensing* 115: 22–36.
20. Lu D, G Li and E Moran (2014) Current situation and needs of change detection techniques. *International Journal of Image and Data Fusion*, 5(1): 13–38.
21. Shi L C and B L Lu (2013) EEG-based vigilance estimation using extreme learning machines. *Neurocomputing* 102: 135–143.
22. Jensen J R (1996) Introductory digital image processing: a remote sensing perspective.
23. Fonte CC, See L, Laso-Bayas JC, Lesiv M, Fritz S (2020) Assessing the accuracy of land use land cover (lulc) maps using class proportions in the reference data. *ISPRS Annals of the Photogrammetry, Remote Sensing and Spatial Information Sciences* 5(3):669-74.
24. Chowdhury M S (2024) Comparison of accuracy and reliability of random forest, support vector machine, artificial neural network and maximum likelihood method in land use/cover classification of urban setting. *Environmental Challenges* 14, 100800.
25. Zhou T, Li Z and Pan J (2018) Multi-feature classification of multi-sensor satellite imagery based on dual-polarimetric sentinel-1A, landsat-8 OLI, and hyperion images for urban land-cover classification. *Sensors*, 18(2): 373.
26. Hegde A S, Ranjan R and Hegde S S (2024) Crop classification and cropping intensity estimation using geospatial technology in the upper Gangetic plains of Uttarakhand. *Heliyon*, 10(22).
27. Katherasala S, Bheenaveni R S, Chinthakindi P, Vadlakonda D, Kummari N and Bandi S S (2024) Unveiling the Detrimental Impacts of Intensive Chemical Use and Monoculture on Soil Health and Sustainable Development Goal 15: Life on Land in Telangana. *Journal of Lifestyle and SDGs Review* 4(2): 10-47172.